Clays and Clay Minerals, Vol. 50, No. 1, 56–62, 2002.

HYDROXYL-STRETCHING BANDS IN POLARIZED MICRO-RAMAN SPECTRA OF ORIENTED SINGLE-CRYSTAL KEOKUK KAOLINITE

S. SHOVAL[1,*], S. YARIV[2], K. H. MICHAELIAN[3], M. BOUDEULLE[4] AND G. PANCZER[4]

[1] Geology Group, Department of Natural Sciences, The Open University of Israel, 16 Klausner Street, 61392 Tel Aviv, Israel

[2] Department of Inorganic and Analytical Chemistry, The Hebrew University of Jerusalem, 91904 Jerusalem, Israel

[3] Natural Resources Canada, CANMET Western Research Centre, Devon Alberta, Canada, T9G 1A8

k[4] LPCML, UMR 5620 CNRS, Claude Bernard University - Lyon 1, 43 Bd 11 November 1918, 69622 Villeurbanne Cedex, France

Abstract—Polarized micro-Raman spectra of a single large crystal of Keokuk kaolinite were recorded in the OH-stretching region with the laser beam directed along the different crystal axes. The Raman spectra are characterized by five OH-stretching bands at 3694, 3683, 3668, 3650 and 3620 cm^{-1} labeled A, Z, B, C and D, respectively. The relative intensities of these five bands depend on the orientation of the crystal and the scattering geometry. The spectra agree with the assertion that bands A and Z arise from out-of-plane vibrations, whereas band D corresponds to an in-plane vibration.The area ratios of the various bands were calculated from fitted curves of spectra recorded with the electric vector of the laser beam parallel to different crystallographic planes. The increments in the relative areas of bands B and C were parallel to those of bands A and Z and it appears that out-of-plane vibrations made considerable contributions to these bands also. From the change of area ratios with the change in the direction of the electric vector of the laser beam, bands A and Z were attributed to LO and TO frequencies of one inner-surface hydroxyl vibration. Bands A + Z, B, C and D were attributed to the vibrations of the hydroxyls assigned by Bish (1993) as OH(3), OH(4), OH(2) and OH(1), respectively. These observations were supported by photoacoustic and transmission IR spectra.

Key Words—Hydroxyl Groups, IR Spectra, Kaolinite, Raman Spectra, SEM Micrographs.

INTRODUCTION

Transmission infrared (IR) spectra of polycrystalline kaolinite exhibit four prominent OH-stretching bands at ~3696, 3670, 3650 and 3620 cm^{-1} (Johnston *et al.*, 1990). Proceeding from high to low frequency, these features were labeled A, B, C and D by Miller and Oulton (1970). About a decade later, a fifth OH band was observed at 3680–3690 cm^{-1} in Raman spectra of kaolinites by several groups (Wiewióra *et al.*, 1979; Johnston *et al.*, 1985; Michaelian, 1986; Frost, 1995; Shoval *et al.*, 1995; Frost *et al.*, 1996) This band, subsequently labeled Z (Michaelian *et al.*, 1991a), was also detected in photoacoustic (Michaelian, 1990) and transmission IR spectra of kaolinites with a high Hinckley index (Shoval *et al.*, 1999a).

Shoval *et al.* (1995) studied the relationship between the textures of altered magmatic rocks from Makhtesh Ramon, Israel, and the Raman spectra of their kaolinites. Band A is prominent near 3700 cm^{-1} in Raman spectra of kaolinite in the altered phenocryst, whereas band Z at ~3688 cm^{-1} predominates in spectra of the altered groundmass. These spectroscopic features were attributed to the crystal size of the kaolinite observed in SEM images. The crystal size of the kaolinite in the altered phenocryst is limited to 1 μm and that of the altered groundmass extends up to 3 μm. Using curve-fitting calculations for IR and Raman spectra, we recently showed that the intensity of band Z relative to band A, and the band area ratio $S_Z/(S_Z+S_A)$, depend on crystal size and the degree of crystallinity of the kaolinite (Shoval *et al.*, 1999a,b). The intensity and area ratio are greater in spectra of large particles with a high degree of crystallinity (high Hinckley index), and lower in spectra of small particles with a low degree of crystallinity.

The most satisfactory explanation for the appearance of band Z in Raman spectra of kaolinites consisting of large particles was given recently by Farmer (1998, 2000). It is known that macroscopic crystals larger than the wavelength of the exciting radiation possess two long-wavelength crystal vibrations, termed longitudinal optic (LO) and transverse optic (TO) modes; both are associated with the same unit-cell vibration in which the dipole moment is generated. The LO modes have higher frequencies than TO modes. According to Farmer (1998, 2000), in thin platy crystals of kaolinite where the thickness of the plates is much less than the wavelength of the impinging beam, vibrations perpendicular to the plates produce bands at their LO frequencies, while those parallel to the plates exhibit TO frequencies. This is the case in the IR spectroscopy study. On the other

* E-mail address of corresponding author: shoval@oumail.openu.a c.il

hand, when coherent plates have a size larger than the wavelength of the propagating beam, both modes may be active in the spectra. This is the case in Raman spectroscopy where the wavelength of the laser beam is in the visible region.

Recently, Shoval *et al.* (1999b) demonstrated that band Z at ~3686 cm^{-1} (TO frequency) is indeed stronger in Raman spectra of highly crystallized kaolinites with large coherent domains. In this paper we describe a micro-Raman spectrum of a single crystal of Keokuk kaolinite. The large crystal size of this kaolinite permits measurements of the micro-Raman spectrum of a single crystal, with the laser beam directed along the different crystal axes.

EXPERIMENTAL

Keokuk kaolinite from geodes in the Mississippian Warsaw Formation near Keokuk, Iowa, USA was kindly provided by W.D. Keller (Hayes, 1963; Keller *et al.*, 1966).

Scanning electron microscopy (SEM) micrographs were obtained using a JEOL (JSM-840) instrument; micro-Raman spectra using a Dilor XY micro-Raman spectrometer; photoacoustic IR spectra using a Bruker IFS 113v spectrometer and a Princeton 6003 photo-acoustic cell; transmission IR spectra using a Nicolet FT-IR spectrometer. These methods were described previously (Shoval *et al.*, 1999a,b). The scattering geometry is similar to that described by Johnston *et al.* (1998).

Curve fitting

The Raman and IR spectra were analyzed with the peak-fitting function in 'Grams' (Galactic) software. Lorentzian shapes were used for the OH bands. Multiple points on either side of the region of interest were used for baseline linearization. Frequencies, widths and the areas of the bands were calculated with this software (Shoval *et al.*, 1999b).

Orientation

The directions of the *a* and *b* crystallographic axes in the kaolinite crystal were determined according to the elongation habit of the plates in the sample examined. To obtain single-crystal Raman spectra with the beam along the *c* axis, the crystal was placed with the (001) face parallel to the *XY* plane of the microscope stage. By rotating the microscopic table the plates were arranged so that the electric vector was along the *a* or *b* axis, yielding the *c*(*aa*)-*c* or *c*(*bb*)-*c* spectrum, respectively. To obtain Raman spectra with the beam along the *b* axis, the (010) face with the cleavage traces of the euhedral crystal was placed parallel to the *XY* plane of the microscope stage. In these measurements the electric vector was along the *c* or *a* axis, giving *b*(*cc*)-*b* or *b*(*aa*)-*b*, respectively. In our system it was impossible to obtain Raman spectra with excitation along the *a* axis. For this purpose the edges between the two faces (110) of the euhedral crystal must be placed on the microscope table. In practice, this was impossible.

RESULTS AND DISCUSSION

Particle size and crystallinity of the Keokuk kaolinite

The SEM micrographs of representative euhedral Keokuk kaolinite crystals are shown in Figure 1. Elongated hexagonal plates are observed when viewing along the *c* axis (Figure 1a). Axis *a* is parallel to the longer (010) face of the crystal, whereas axis *b* is perpendicular. The sizes of the hexagonal plates extend up to 6.0–10.0 μm along the *a* axis and 3.0–7.0 μm along the *b* axis. The lengths of their sides are 2.0–6.0 μm. The height of most crystals in the *c* axis direction extends up to 10–15 μm. A book-type structure, in which coherent plates are separated by

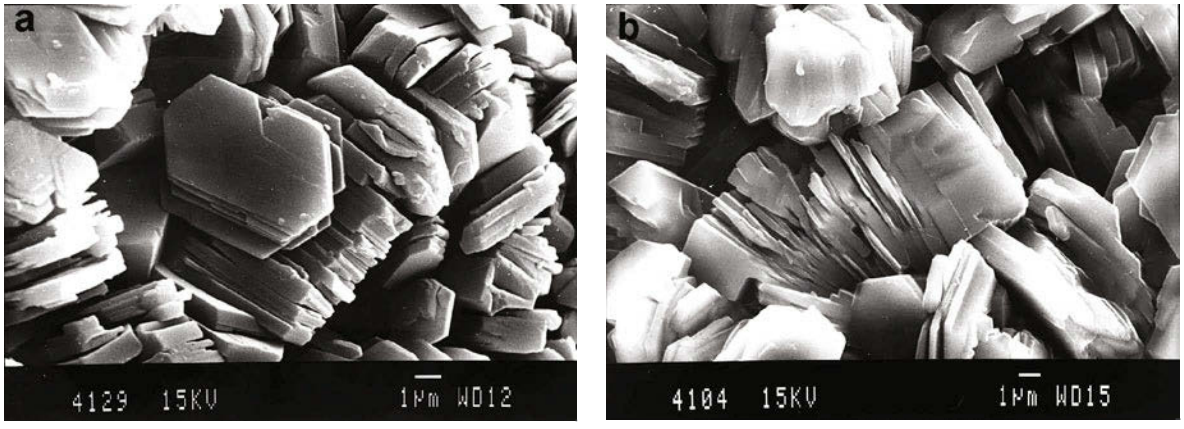

Figure 1. SEM micrographs of representative euhedral Keokuk kaolinite crystals. (a) View along the crystallographic *c* axis, illustrating elongated hexagonal plates. Axis *a* is parallel to the longer (010) face of the crystal, whereas axis *b* is perpendicular. (b) View along *b* or *a* axes displaying a book-type structure, in which coherent plates are separated by cleavage.

https://doi.org/10.1346/000986002761002676 Published online by Cambridge University Press

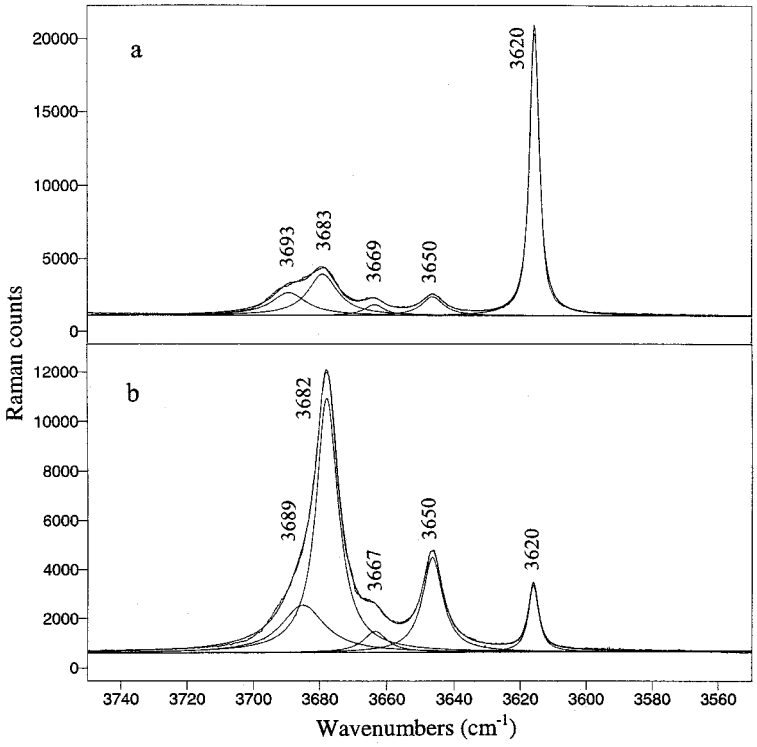

Figure 2. Curve-fitted polarized micro-Raman spectra of oriented single-crystal Keokuk kaolinite in the OH-stretching region, collected with the laser beam propagating along the crystallographic *b* axis (parallel to the kaolinite plates). (a) *b(aa)-b*; (b) *b(cc)-b* Raman scattering geometries.

cleavage planes, is observed in the views along the *b* or *a* axes (Figure 1b). The thickness of the coherent plates between the cleavage trace in many crystals extends up to 2.5–3.0 μm, but in some crystals only to ~0.25–1.0 μm.

RAMAN SPECTRA

To describe the scattering geometry for different orientations of the crystallographic axes, we used the Porto notation (Swanson, 1973), adapted by Johnston *et al.* (1998) for the Raman spectrum of a single crystal of dickite.

Polarized Raman spectra of a single crystal of the Keokuk kaolinite specimen in the OH-stretching region, recorded with different crystal orientations, are shown in Figures 2 and 3 together with the curve-fitting results. Spectra were obtained with VV (vertical-vertical) polarizations, *i.e.* the polarizations of the incident laser beam and the scattered light were parallel. The spectra are plotted in these figures such that the most intense band is full-scale in each case (autoscale). Summarizing the findings, the Raman spectra are characterized by five OH-stretching bands at 3694, 3683, 3668, 3650 and 3620 cm^{-1}, labeled A, Z, B, C and D, respectively. The relative intensities of these five bands depend strongly on the orientation of the crystal and the scattering geometry.

Polarized micro-Raman spectra recorded with the laser beam along the *b* axis are depicted in Figure 2. The electric vector was along the *a* axis *b*(*aa*)-*b*, or along the *c* axis *b*(*cc*)-*b*. When the peak intensities of the *b*(*aa*)-*b* experiment are compared with those of *b*(*cc*)-*b* it is obvious that bands A and Z are very weak in the former and highly intensified in the latter. On the other hand, band D, which is the most intense band in the former spectrum, becomes weak in the latter. These observations agree with the assertion that bands A and Z arise from out-of-plane vibrations, whereas band D corresponds to an in-plane vibration. Considering bands B and C, the intensities of these bands increase significantly from *b*(*aa*)-*b* to *b*(*cc*)-*b*. Raman spectra recorded with the laser beam directed along the *c* axis are depicted in Figure 3. As one would expect, these spectra showed out-of-plane band D to be very intense, and the other bands to be very weak.

The area ratios $S_Z/(S_Z+S_A)$, where S_Z and S_A are the areas of bands Z and A, respectively, were calculated from curve-fitting data for the Raman spectra (Table 1). These area ratios are greater when the direction of the beam is parallel to the layer (along crystallographic axis *b*) and less when the direction of the beam is perpendicular to the aluminosilicate layer (along crystallographic axis *c*). We interpret the relationship between band and intensity and crystal orientation in terms of LO and TO modes of crystal vibration. When the beam is

https://doi.org/10.1346/000986002761002676 Published online by Cambridge University Press

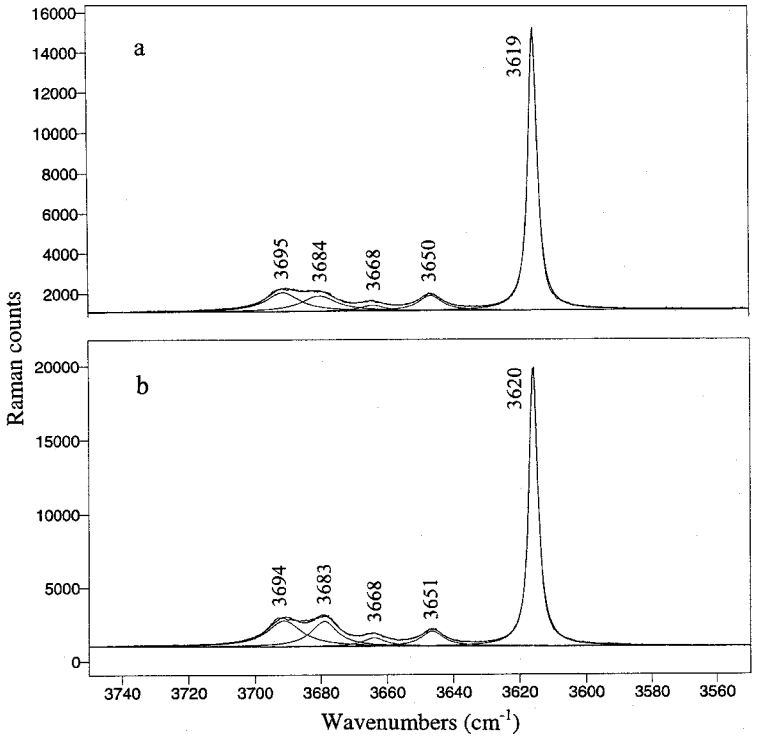

Figure 3. Curve-fitted polarized micro-Raman spectra of oriented single crystal Keokuk kaolinite in the OH-stretching region, collected with the laser beam propagating along the crystallographic *c* axis (perpendicular to the kaolinite plates). (a) *c(aa)-c*; (b) *c(bb)-c* Raman scattering geometries.

normal to the plane, the behavior of the spectra is controlled by the thickness of the layer, which is slightly greater than the wavelength of the laser. Bands A (LO frequency) and Z (TO frequency) are observed in the resulting spectrum but the ratio of Z to A is small. When the beam propagates along the plane, the particle behaves as a macrocrystal with a size much larger than the wavelength, and the TO frequency is much more intense than the LO frequency.

Area ratios S_A/S_D, S_Z/S_D, S_B/S_D and S_C/S_D are collected in Table 1. Comparing these ratios in spectra recorded with the electric vector parallel to the (001) plane [*b(aa)-b*, *c(aa)-c* and *c(bb)-c*] with that recorded with the electric vector normal to this plane [*b(cc)-b*] shows an increase of this ratio by a factor of 9–20. These ratios should be considered only as trends. No analysis of the local Raman tensor was carried out during calibration of the system response, but since these ratios are confined to a narrow wavenumber range it is expected that any inaccuracy is small. It should be noted that the area of band D also depends on the direction of the electric vector of the incident light. It is large when the electric vector is in the clay plane and becomes small when it is out-of-plane. Since band D is the denominator in these ratios, the

Table 1. Curve-fitting data of micro-Raman spectra, photoacoustic IR spectrum and transmission IR spectrum (KBr disk) of single-crystal Keokuk kaolinite in the OH-stretching region. The relative intensities of the bands A and Z are demonstrated by the area ratios $S_Z/(S_Z+S_A)$, where *S* is the area of a peak obtained by curve-fitting calculations. The intensities of bands A, Z, B and C with respect to band D are demonstrated by the area ratios S_A/S_D, S_Z/S_D, S_B/S_D and S_C/S_D.

Spectra	Polarizaton direction	$S_Z/(S_Z+S_A)$	S_A/S_D	S_Z/S_D	S_B/S_D	S_C/S_D	χ^2	RMS*
Raman spectra								
b(aa)-b	VV	0.62	0.27	0.45	0.08	0.14	0.06	522
b(cc)-b	VV	0.73	2.89	8.13	0.73	2.76	0.29	109
c(aa)-c	VV	0.46	0.27	0.23	0.06	0.15	0.03	400
c(bb)-c	VV	0.48	0.36	0.34	0.17	0.23	0.02	501
Photoacoustic IR spectra	Unground	0.43	0.73	0.56	0.89	0.97	9.80	0
Transmission IR spectra	Ground slightly	0.41	1.32	0.91	0.48	0.55	1.86	0
	Ground extensively	0.19	2.04	0.49	0.52	0.41	0.99	0

* Root mean square

https://doi.org/10.1346/000986002761002676 Published online by Cambridge University Press

increments in the area of bands A, Z, B and C observed by changing the direction of the electric vector should be smaller than the factors 9–20. But since the increments in the relative areas of bands B and C are parallel to those in the relative areas of bands A and Z, it appears that these bands, like bands A and Z, have significant contributions by out-of-plane vibrations.

The crystal structure of Keokuk kaolinite at 1.5 K was determined using neutron powder diffraction and Rietveld refinement by Bish (1993). He labeled OH groups that form angles with the (001) plane of 0.38, 73.16, 68.24 and 60.28° as OH(1), OH(2), OH(3) and OH(4), respectively. In the layered kaolinite structure with the laser beam along the *b* axis, the intensities of the OH bands depend on the orientation of the electric vector of the beam and on the angles between the direction of the OH group and the (001) plane. With the electric vector along the *a* axis the OH band intensifies with decreasing angle because of increasing projection of the OH vibration on this axis. With the electric vector along the *c* axis, the OH band intensifies with increasing angle because of increasing projection of the OH vibration along this axis. From the change of the area ratios with the change in the direction of the electric vector of the laser beam shown in Table 1, it appears that bands A + Z, B, C and D are due to OH-stretching vibrations OH(3), OH(4), OH(2) and OH(1), respectively. According to Farmer (1998), there is a high degree of coupling between OH groups 2, 3 and 4. In this case the very low intensity of band B is explicable by a coupled antiphase vibration, where the change in polarizability along *c* produced by one OH group is canceled by the other.

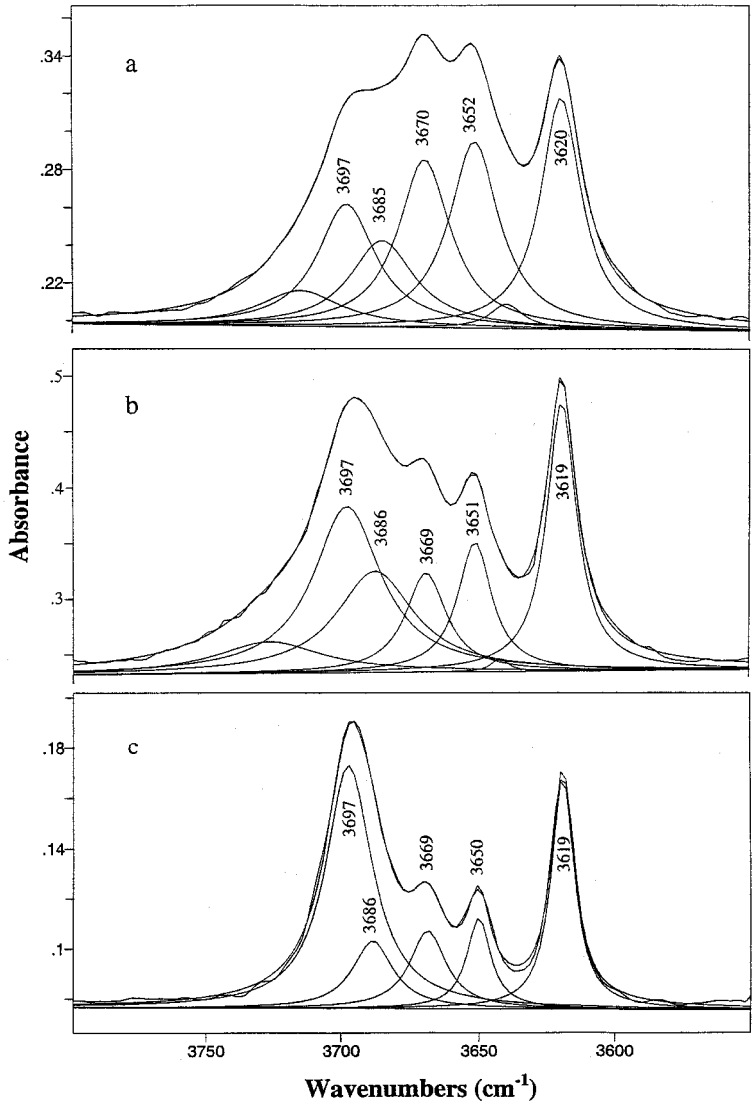

Figure 4. Curve-fitted spectra of the Keokuk kaolinite in the OH-stretching region. (a) Photoacoustic spectrum; (b) transmission IR spectrum in a KBr disk after slight grinding; (c) transmission IR spectrum after re-grinding and re-pressing five times.

https://doi.org/10.1346/000986002761002676 Published online by Cambridge University Press

Photoacoustic and transmission IR spectra

Curve-fitted photoacoustic and transmission IR spectra of Keokuk kaolinite in the OH-stretching region are illustrated in Figure 4. All five bands A, Z, B, C and D are observed in the curve-fitted spectra, but band A is more intense than band Z (Shoval *et al.*, 1999a,b).

In the photoacoustic method, the Keokuk kaolinite was examined unground and the result can be considered as a representative IR spectrum of several unoriented single crystals. In this sense, it can be compared with the single-crystal Raman spectra discussed above. However, in contrast with the polarized Raman spectra which depend on the orientation of the crystal, the photoacoustic IR spectrum is not known to depend on orientation. It should be noted that the ratios S_B/S_D and S_C/S_D are high in the photoacoustic spectra and small in the Raman and transmission IR spectra compared with the ratios S_A/S_D and S_Z/S_D (Table 1). Photoacoustic spectra arise from the heating effect produced by the absorbed radiation. In large kaolinite crystals, strong absorption bands are associated with high reflectivity over the frequency range LO–TO. Consequently, they produce less heat than the weak absorption bands at 3670 and 3650 cm^{-1}.

Transmission IR spectra of the Keokuk kaolinite were obtained after slight grinding and after extensive grinding, during preparation of the KBr disk. The latter sample was reground and re-pressed five times during the preparation. As a result of the grinding, the intensity of band Z with respect to band A decreased markedly (Table 1). This is in agreement with our previous observation that band Z displays greater intensity in Raman spectra of kaolinites which have large coherent domains (Shoval *et al.*, 1999b).

In the slightly ground sample, band A appears broad in the transmission spectra due to the brief grinding. Increased band sharpness during grinding which is observed in Figure 4c was previously attributed by Yariv (1975a,b) to delamination of the kaolinite domains. As a result of reduced crystal thickness, the 3660 cm^{-1} band becomes less prominent and the 3697 cm^{-1} band becomes more prominent.

CONCLUSIONS

The OH-stretching bands in polarized micro-Raman spectra of single-crystal Keokuk kaolinite were investigated with the laser beam directed along the *b* or *c* axes. The frequencies and areas of the bands were determined by curve fitting. Five bands were observed in the 3620–3700 cm^{-1} region; beginning at high frequency, these features are labeled A, Z, B, C and D, respectively. Bands A and Z can be attributed to the LO and TO frequencies of the vibration of the inner-surface hydroxyls assigned by Bish (1993) as OH(3). The intensity of band Z relative to band A is large when the laser beam propagates along the *b* axis, and small when it is along the *c* axis. We also show that bands B and C are intensified when the electric vector of the laser beam is along *c* (together with bands A and Z), whereas band D is intensified when the electric vector is along axes *a* or *b*. Bands B, C and D are attributed to the vibrations of the hydroxyls assigned by Bish (1993) as OH(4), OH(2) and OH(1), respectively.

ACKNOWLEDGMENTS

We wish to thank an anonymous referee for suggestions on the interpretation of the different spectra. This work was supported by the Open University of Israel Research Fund. This support is gratefully acknowledged.

REFERENCES

Bish, D.L. (1993) Rietveld refinement of the kaolinite structure at 1.5 K. *Clays and Clay Minerals*, **41**, 738–744.

Bish, D.L. and Johnston, C.T. (1993) Rietveld refinement and Fourier transform infrared spectroscopic study of the dickite structure at low temperature. *Clays and Clay Minerals*, **41**, 297–304.

Farmer, V.C. (1998) Differing effects of particle size and shape in the infrared and Raman spectra of kaolinite. *Clay Minerals*, **33**, 601–604.

Farmer, V.C. (2000) Transverse and longitudinal crystal modes associated with OH stretching vibrations in single crystals of kaolinite and dickite. *Spectrochimica Acta A*, **56**, 927–930.

Frost, R.L. (1995) Fourier transform Raman spectroscopy of kaolinite, dickite and halloysite. *Clays and Clay Minerals*, **43**, 191–195.

Frost, R.L., Fredericks, P.M. and Shurvell, H.F. (1996) Raman microscopy of some kaolinite clay minerals. *Canadian Journal of Applied Spectroscopy*, **41**, 10–14.

Hayes, J.B. (1963) Kaolinite from Warsaw geodes, Keokuk region, Iowa. *Iowa Academy of Sciences*, **70**, 261–272.

Johnston, C.T., Sposito, G. and Birge, R.R. (1985) Raman spectroscopic study of kaolinite in aqueous suspension. *Clays and Clay Minerals*, **33**, 483–489.

Johnston, C.T, Agnew, S.F. and Bish, D.L. (1990) Polarized single-crystal Fourier-transform infrared microscopy of Ouray dickite and Keokuk kaolinite. *Clays and Clay Minerals*, **38**, 573–583.

Johnston, C.T., Helsen, J., Schoonheydt, R.A., Bish, D.L. and Agnew, S.F. (1998) Single-crystal Raman spectroscopic study of dickite. *American Mineralogist*, **83**, 75–84.

Keller, W.D., Pickett, E.E. and Reesman, A.L. (1966) Elevated dehydroxylation temperature of the Keokuk geode kaolinite – a possible reference mineral, Pp. 75–85 in: *Proceedings of the International Clay Conference, Jerusalem*, Vol. 1 (L. Heller and A. Weiss, editors). Israel Program for Scientific Translations, Jerusalem.

Michaelian, K.H. (1986) The Raman spectrum of kaolinite #9 at 210°C. *Canadian Journal of Chemistry*, **64**, 285–289.

Michaelian, K.H. (1990) Step-scan phtoacoustic infrared spectra of kaolinite. *Infrared Physics*, **30**, 181–186.

Michaelian, K.H., Yariv, S. and Nasser, A. (1991a) Study of the interactions between cesium bromide and kaolinite, by photoacoustic and diffuse reflectance infrared spectroscopy. *Canadian Journal of Chemistry*, **69**, 749–754.

Michaelian, K.H., Friesen, W.I., Yariv, S. and Nasser, A. (1991b) Diffuse reflectance infrared spectra of kaolinite and kaolinite/alkali halide mixtures. Curve-fitting of the OH stretching region. *Canadian Journal of Chemistry*, **69**, 1786–1790.

Miller, J.G. and Oulton, J.D. (1970) Prototropy in kaolinite during percussive grinding. *Clays and Clay Minerals*, **18**, 313–323.

Shoval, S., Boudeulle, M., Panczer, G. and Yariv, S. (1995) Raman micro-spectrometry and infrared spectroscopy study of the alteration products of trachyte sills and dykes in Makhtesh Ramon area, Israel. Pp. 325–337 in: *Physics and Chemistry of Dykes* (G. Baer and A. Heimann, editors). Balkema, Rotterdam, The Netherlands.

Shoval, S., Yariv, S., Michaelian, K.H., Lapides, I. Boudeulle, M., Panczer, G. (1999a) A fifth OH-stretching band in IR spectra of kaolinites. *Journal of Colloid and Interface Science*, **212**, 523–529.

Shoval, S., Yariv, S., Michaelian, K.H., Boudeulle, M. and Panczer, G, (1999b) Hydroxyl-stretching bands 'A' and 'Z' in Raman and infrared spectra of kaolinites. *Clay Minerals*, **34**, 551–563.

Swanson, B.I. (1973) General notation for polarized Raman scattering from gases, liquids, and single crystals. *Applied Spectroscopy*, **27**, 382–385.

Wiewióra, A., Wieckowski, T. and Sokolowska, A. (1979) The Raman spectra of kaolinite subgroup minerals and of pyrophyllite. *Archiwum Mineralogiczne*, **35**, 5–14.

Yariv, S. (1975a) Some effect of grinding kaolinite with potassium bromide. *Clays and Clay Minerals*, **23**, 80–82.

Yariv, S. (1975b) Infrared study of grinding kaolinite with alkali metal chlorides. *Powder Technology*, **12**, 131–138.

(*Received 20 May 2000; revised 8 June 2001; Ms. 452*)